sustainable chemistry

MDPI

Perspective

A Perspective on Solar-Driven Electrochemical Routes for Sustainable Methanol Production

Aaditya Pendse † and **Aditya Prajapati *,†**

Materials Science Division (MSD), Lawrence Livermore National Laboratory, Livermore, CA 94550, USA
* Correspondence: prajapati3@llnl.gov
† These authors contributed equally to this work.

Abstract: The transition towards sustainable and renewable energy sources is imperative in mitigating the environmental impacts of escalating global energy consumption. Methanol, with its versatile applications and potential as a clean energy carrier, a precursor chemical, and a valuable commodity, emerges as a promising solution within the realm of renewable energy technologies. This work explores the integration of electrochemistry with solar power to drive efficient methanol production processes, focusing on electrochemical reduction (ECR) of CO_2 and methane oxidation reaction (MOR) as pathways for methanol synthesis. Through detailed analysis and calculations, we evaluate the thermodynamic limits and realistic solar-to-fuel (STF) efficiencies of ECR and MOR. Our investigation encompasses the characterization of multijunction light absorbers, determination of thermoneutral potentials, and assessment of STF efficiencies under varying conditions. We identify the challenges and opportunities inherent in both ECR and MOR pathways, shedding light on catalyst stability, reaction kinetics, and system optimization, thereby providing insights into the prospects and challenges of solar-driven methanol synthesis, offering a pathway towards a cleaner and more sustainable energy future.

Keywords: methanol production; solar-driven electrochemistry; renewable energy integration; electrochemical reduction of CO_2; methane oxidation reaction; solar-to-fuel efficiency

check for updates

Citation: Pendse, A.; Prajapati, A. A Perspective on Solar-Driven Electrochemical Routes for Sustainable Methanol Production. *Sustain. Chem.* **2024**, *5*, 13–26. https://doi.org/10.3390/suschem5010002

Academic Editors: Jan-Willem Bos and Francesca Deganello

Received: 30 January 2024
Revised: 1 March 2024
Accepted: 4 March 2024
Published: 6 March 2024

1. Introduction

The escalating global population, coupled with the surging energy demands projected by the International Energy Agency, necessitates a paradigm shift towards sustainable and renewable energy sources. Current trends, as indicated by the energy progress report, reveal that a substantial 85.33% [1] of the world's energy consumption is derived from non-renewable sources, contributing to alarming levels of carbon dioxide emissions. While renewable resources, including wind and solar power, have witnessed a commendable surge, constituting 12.84% of global energy consumption in 2021 [2], challenges persist. The intermittent nature of solar and wind energy, along with the logistical hurdles in large-scale electricity storage and transmission, underscores the imperative for alternative solutions [3]. Hydrogen, touted as a clean fuel, faces practical limitations due to storage complexities and high costs [4]. In this context, the methanol economy emerges as a promising avenue [5,6]. Methanol, with its single carbon structure, liquid state at room temperature, and diverse applications, offers a compelling solution to store surplus energy efficiently. Unlike hydrogen, methanol can seamlessly integrate into existing infrastructure, making it a viable and practical choice for a sustainable energy future. Moreover, methanol's versatility extends beyond its role as a fuel [3]. Its high-octane number makes methanol an ideal additive to gasoline, offering a cleaner and more environmentally friendly option for the transportation sector. Additionally, methanol serves as a critical precursor and commodity chemical for numerous industries, including plastics, textiles, pharmaceuticals, and agriculture. Its versatility as a feedstock allows for the production of a wide array of

essential products [7], thereby contributing to various sectors of the economy. In addition to its role as a critical precursor and commodity chemical for numerous industries, methanol's versatility extends to the realm of energy storage and utilization. Methanol serves as a vital component in direct methanol fuel cells (DMFCs), offering a clean and efficient means of electricity generation [8]. DMFCs harness the electrochemical oxidation of methanol to produce electricity, providing a promising avenue for decentralized power generation and mobile applications. By embracing methanol as a cornerstone of the renewable energy transition, we unlock its potential as a sustainable precursor for a multitude of industries, paving the way for a greener and more resilient future.

The utilization of electrochemistry, harnessing the power of affordable electrons to drive chemical reactions, emerges as a highly attractive and innovative approach within the methanol economy. This method holds the promise of transforming renewable energy, particularly solar energy, into a potent driver for sustainable chemical processes. By coupling electrochemistry with solar energy, we unlock a synergistic relationship that not only addresses the intermittent nature of sunlight but also enhances the overall efficiency of energy conversion. Solar-driven electrochemical processes offer a pathway to utilize abundant and cost-effective electrons, providing a clean and renewable energy source for the production of methanol. An electrochemical system is primarily integrated with solar energy in two different ways: (1) coupling of a photovoltaic (PV) cell with an independent electrochemical cell (PV–EC) [9,10]. (2) Incorporating a photoelectrocatalyst (PEC) in an electrochemical system [11,12]. While a PEC offers a compact design and uses fewer materials compared to a PV–EC system, PECs to date have been limited by their efficiency to out-compete PV–EC systems for higher throughput [13]. Considerable efforts have also been devoted to achieving the solar-driven electrochemical conversion of methane/CO_2 to methanol through photocatalysis [14–17] incorporating a PEC system. The efficient functioning of a photocatalyst involves absorption units for initial light absorption, generating electron–hole pairs, and active centers that facilitate methane/CO_2 activation, leading to methanol production. This coupled approach, using a single photocatalyst for both functions, is cost-effective and compact, but limits the selection of optimal absorber and catalyst in a PEC system. The decoupled approach, using independent components in PV–EC systems, offers flexibility but tends to be costlier, as it allows the selection of the best absorber and catalyst separately, enhancing efficiency at a higher cost. Either of these integrations, however, are still advantageous to implement compared to a standalone electrochemical system to reduce the carbon footprint of such processes. Solar integration not only contributes to the reduction of greenhouse gas emissions, but also aligns with the broader goals of creating a circular and sustainable energy ecosystem.

A multitude of methods, spanning thermochemical [18,19], electrochemical [20–22], photoelectrochemical [23,24], and photocatalytic [25,26] reactions, have been explored for the reduction of CO_2 into valuable fuels. Among these, electrochemical reduction (ECR) of CO_2 emerges as the most promising due to its distinct advantages [27]. The conversion of CO_2 to CH_3OH through electrochemical means is particularly noteworthy, given its environmental sustainability and its potential role in establishing a methanol economy. Notably, Jouny et al. conducted a techno-economic analysis of ECR technology, indicating the feasibility of large-scale production of carbon monoxide (CO) and formic acid (HCOOH) [28]. The identified ECR reaction pathways for CO_2 to CH_3OH conversion involve complexities related to catalyst stability and reaction kinetics [29–31]. However, extensive research into the different types of electrocatalysts and novel electrolysis techniques promises the commercial viability of the ECR technology. Transition metals and their compounds, notably metal complexes and alloys, are extensively studied as electrocatalysts in CO_2 electrochemical reduction due to their favorable electronic properties [29]. Additionally, reports on the electrochemical reduction of CO_2 over semiconductor electrodes and photocatalysts expand the scope, producing not only CH_3OH but also other valuable products [32,33]. Additionally, researchers are increasingly focusing on solar power-driven electrochemical reduction of CO_2 to methanol. Barton et al. demonstrated selective solar-

driven reduction of CO_2 to methanol using a catalyzed p-GaP-based photoelectrochemical cell with a quantum efficiency of 41% under 365 nm illumination [34]. Other studies have explored solar-driven photoelectrochemical reduction of CO_2 to methanol using various photocathodes, showcasing high faradaic efficiencies and low overpotentials [35,36]. This ongoing research collectively underscores the potential of electrochemical approaches, both traditional and solar-driven, in paving the way for a sustainable and efficient pathway from CO_2 to methanol, offering insights into both fundamental reaction mechanisms and practical applications. This positive progression in research of the ECR technology has also been confirmed by recent successful demonstrations of commercial-scale and cost-effective methanol production by companies like Shunli [37] and Oxylus Energy [38].

Parallel to the progress in reducing CO_2 to methanol, methane oxidation reaction (MOR) to methanol has surfaced as a promising pathway for efficient methanol production. Electrochemical strategies, particularly those operational at low to mild temperatures, have garnered attention for their potential [39,40]. MOR to methanol represents a sustainable approach with multifaceted environmental benefits. Methane, a potent greenhouse gas with a global warming potential 23 times higher than CO_2, poses a significant environmental challenge. By converting methane to methanol, not only can we mitigate its detrimental impact on climate change, but we can also address the issue of methane flaring, where excess methane is simply burned, contributing to additional CO_2 emissions. Leveraging methane, a decentralized resource, for methanol production offers a compelling solution, tapping into existing methane sources while reducing dependence on fossil fuels. Furthermore, methanol's characteristics as a safe and convenient transporter make it an attractive alternative to compressed methane, enhancing its potential as a sustainable energy carrier. Through electrochemical methane oxidation, we not only curb greenhouse gas emissions but also unlock the potential of methane as a renewable feedstock, ushering in a more sustainable era of chemical synthesis and energy utilization. In that framework, Mustain et al. utilized a mixed oxide catalyst of NiO/ZrO_2 at room temperature, showcasing its efficacy in converting CH_4 to various oxygenates [41]. Sun et al. reported a CH_3OH production rate of 25 μmol/gcat/h with a Faradaic efficiency of 89% using a NiO/Ni catalyst at room temperature [42]. Surendranath et al. achieved a production rate of 268 μmol/gcat/h and a selectivity of 69% using the Pt(II):Pt(IV) catalyst [43]. Transition metal oxides, including NiO/ZrO_2, $Ni(OH)_2/ZrO_2$, and Co_3O_4/ZrO_2, have been investigated for room temperature electrochemical oxidation of methane in carbonate-based systems [41,44,45]. The utilization of membrane electrode assemblies (MEAs) in methanol production has shown promise, allowing for advanced control over catalyst environments and selective reactant transport. Moreover, akin to CO_2 reduction, solar-driven methane oxidation to methanol has garnered attention. Moon et al. demonstrated a solar cell-powered electrochemical CH_4 conversion, achieving an energy-efficient and environmentally friendly process that produced 7165.0 μmol/gcat of CH_3OH at ambient pressure and 21,986.6 μmol/gcat at 10 bar pressure in a 12 h reaction [46]. These collective advancements underscore the multifaceted and evolving landscape in electrochemical methane oxidation, contributing to the diversification of sustainable methanol synthesis methodologies. Owing to the low rates of methanol production in both the ECR and MOR technologies, it is also imperative that robust experimental protocols are established for analyzing the catalyst performance. Standardized reaction parameters such as temperature, pressure, and reactant concentrations must be precisely maintained. Comprehensive characterization methods, including spectroscopic and microscopic analyses, should be employed to understand catalyst morphology and identify active sites. Control experiments, such as blank runs or use of inert materials should be conducted to help discern genuine catalytic effects from external factors. Additionally, ensuring reproducibility through repeated trials is vital for establishing the reliability of observed results. These protocols collectively contribute to the accurate evaluation of catalyst performance, promoting consistency and comparability across different studies in the pursuit of advancing sustainable methanol production processes. In general, the robust practices are even more important with additional complexity

of coupling electrochemical processes such as the ones discussed in this work with either a photoelectrocatalyst (PEC) or a photo-voltaic (PV) system. Some of the crucial best practices are highlighted in the works by Bonchio et al. [47], and Seger et. al [48], addressing the complexity of different electrochemical systems.

Schematics of typical aqueous electrochemical systems used in the literature showing ECR and MOR are shown in Figure 1. Since these are aqueous electrochemical systems, the methanol producing reactions from both ECR and MOR are also competing with hydrogen evolution reaction (HER) on the cathode and oxygen evolution reaction (OER) on the anode. A significant research effort in designing electrocatalysts for such systems is catered towards suppressing these parasitic side reactions for better ECR and MOR performance [49]. As advancements continue in electrochemical systems, aimed at producing methanol from CO_2 or CH_4, it becomes essential to assess their integration with renewable energy sources like solar power. These reactions, driven by electrical energy, stand to benefit from solar energy, further mitigating their carbon footprint. While several efforts have explored utilizing multijunction light absorbers to convert CO_2 into fuels using sunlight [50–53], there is a scarcity of literature on solar-driven CH_4 conversion.

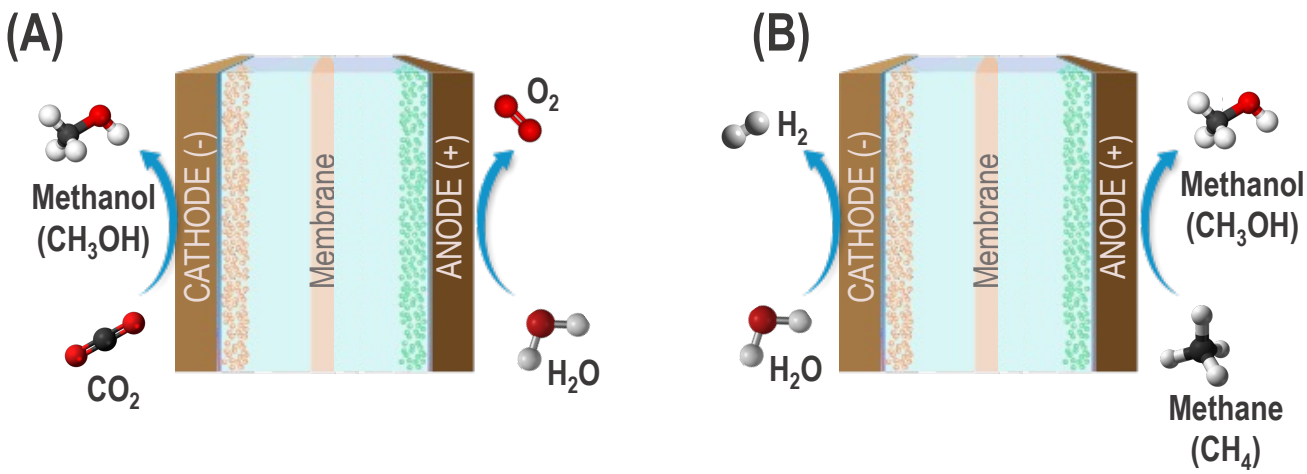

Figure 1. Schematics of typical aqueous electrochemical systems. (**A**) ECR to produce methanol on the cathode while the water oxidation occurs on the anode to produce oxygen. (**B**) MOR to produce methanol on the anode while the water reduction occurs on the cathode to produce hydrogen.

The limited exploration of the solar driven electrochemical processes can mainly be attributed to a number of limitations primarily including: (1) Inadequate performance of the light absorbers. (2) Instability of PEC systems for long duration ECR or MOR in aqueous media. (3) Losses in a PV–EC system associated with direct current to direct current (DC–DC) conversion from PV to EC systems. Hence, there are research efforts focused on circumventing these limitations. The literature predominantly highlights electrocatalyst and photoelectrocatalyst optimization for high efficiency and longevity [54,55], surface modifications, and the development of protective layers are underway [56,57]. Furthermore, electrolyte engineering and exploring advanced electrolysis techniques like tandem catalysis [58–61], and improving electrode designs for to enhance mass transport of the reactant [62] are also being explored. Acknowledging the current scope for progress and the limitations of the solar-driven electrochemical systems, this article aims to serve as a "catalyst" to initiate and expand the research and discussions around solar driven electrochemical methanol production. This article thus aims to offer insights into the thermodynamic and realistic STF efficiency of ECR and MOR as promising pathways for methanol production, fostering a sustainable and circular energy ecosystem. Despite ECR being at a higher Technology Readiness Level (TRL) compared to MOR, it is an opportune moment to evaluate the solar-to-fuel (STF) efficiencies of both processes. The subsequent sections are structured as follows: The Methods section delineates the mathematical expressions for determining Shockley–Queisser (SQ) limits of multijunction light

absorbers, the utilization of thermoneutral potential to describe an ideal electrochemical cell, and the computation of STF efficiencies for ECR and MOR to methanol. The Results and Discussion section examines the current-voltage characteristics of multijunction light absorbers, ideal STF efficiencies for methanol production via ECR and MOR, and realistic STF efficiencies for both pathways. Finally, the Conclusions section offers insights and recommendations for implementing such integration in solar-driven electrochemical methanol production systems.

2. Methods

Current-voltage (JV) characteristics of a Multijunction Light Absorber: We consider ideal, intrinsic light absorbers with up to 5 junctions of optimal bandgaps to assess the performance limits of ideal solar-driven ECR and MOR to methanol. The JV characteristic of each junction in the light absorber is determined by a detailed balance of photons, encompassing thermal generation of carriers, electron-hole recombination, and total absorption of photons with energy exceeding the band gap of the junction. In our ideal condition calculations, we disregard extrinsic losses such as light reflection, contact shadowing, series resistance, inefficient collection of electrons and holes, nonradiative recombination, and temperature rise. The JV characteristics of an ideal multijunction light absorber are derived by applying bias across each junction for a terrestrial air mass (AM) 1.5 spectrum at 1 sun, expressed as follows:

$$V(J) = \frac{kT}{e}\Sigma_{i=1}^{n}\left[\frac{J_{sc,i} - J}{J_{0,i}} + 1\right] \tag{1}$$

where $V(J)$ (Volt) reprecss the light absorber, e (C) denotes the electronic charge, k (JK^{-1}) denotes the Boltzmann constant, T (K) stands for the temperature, n denotes the number of junctions, J (mA cm^{-2}) represents the photocurrent density, $J_{sc,i}$ (mA cm^{-2}) denotes the short-circuit current density of the ith junction, and $J_{0,i}$ (mA cm^{-2}) is the saturation current density of the ith junction. Further details and comprehensive calculations are available in our prior work [63].

Thermoneutral potential: The operation of an ideal electrochemical cell can be conceptualized in two ideal states: equilibrium or adiabatic. The equilibrium potential is defined as:

$$V_{eq} = \frac{\Delta G^0}{nF} = \frac{1}{nF}\left(\Delta H^0 - T\Delta S^0\right) \tag{2}$$

where V_{eq} (Volt) represents the equilibrium potential, ΔG^0 (kJmol^{-1}) denotes the standard Gibbs free energy, ΔH^0 signifies the standard enthalpy, ΔS^0 represents the standard entropy of formation of the electrochemical reaction under consideration, n is the number of electrons per mol of the product formed, and $F = 96,485$ (C mol^{-1}) is the Faraday's constant. It is crucial to note that under equilibrium, an electrochemical cell does not generate a net current and thus, cannot yield a nonzero STF efficiency for any configuration of solar integration with an electrochemical cell. However, an electrochemical cell operating under adiabatic (or isentropic) conditions can produce a net positive current at potentials higher than V_{eq}. This operating potential is termed the thermoneutral potential and is defined as:

$$V_{th} = \frac{\Delta H^0}{nF} \tag{3}$$

where V_{th} represents the thermoneutral potential.

STF efficiency: The STF efficiency is defined as the ratio of power generated as fuel from ECR or MOR to the incident solar power and is expressed as:

$$\eta_{STF}(\%) = \frac{J_{op}\eta_F \times V_{th} \times A_{EC}}{P_s \times A_{LA}} \times 100 \tag{4}$$

where η_{STF} denotes the STF efficiency, η_F represents the Faradaic efficiency of methanol, J_{op} (mA cm^{-2}) signifies the operating current density of the electrochemical cell at a given

potential, $P_s = 100$ (mW cm^{-2}) denotes the average power of solar insolation per unit area for irradiation at the ground level, A_{EC} (cm^2) is the electrode area of the electrochemical cell, and A_{LA} (cm^2) is the area of illumination of the light absorber. Unless mentioned otherwise, the calculations highlighted in this work assume $A_{EC} = A_{LA}$ for simplicity.

3. Results and Discussion

The assessment of the solar integration of any electrochemical system can be initiated with the consideration of the most ideal scenario, namely, determining the thermodynamic limits. In this context, the thermodynamic limits for STF efficiency in methanol production through either ECR or MOR can be assessed by conducting detailed balance calculations for SQ limits to observe the JV characteristics of multijunction light absorbers followed by determining the thermoneutral potentials of ECR and MOR. The SQ limits were determined using Equation (1), and Figure 2 illustrates the JV characteristics of ideal multijunction light absorbers. Notably, the current density decreases with an increase in cell voltage (or electrochemical load) due to a decrease in the fraction of solar radiation absorbed at higher voltages. Additionally, current density decreases with an increase in the number of junctions, a consequence of restrictions imposed by current matching. These JV characteristics emphasize that within the evaluated range of electrochemical load, double and triple junctions exhibit higher current densities across a broader range of cell voltages, making them favorable starting points for the solar integration of any electrochemical reaction.

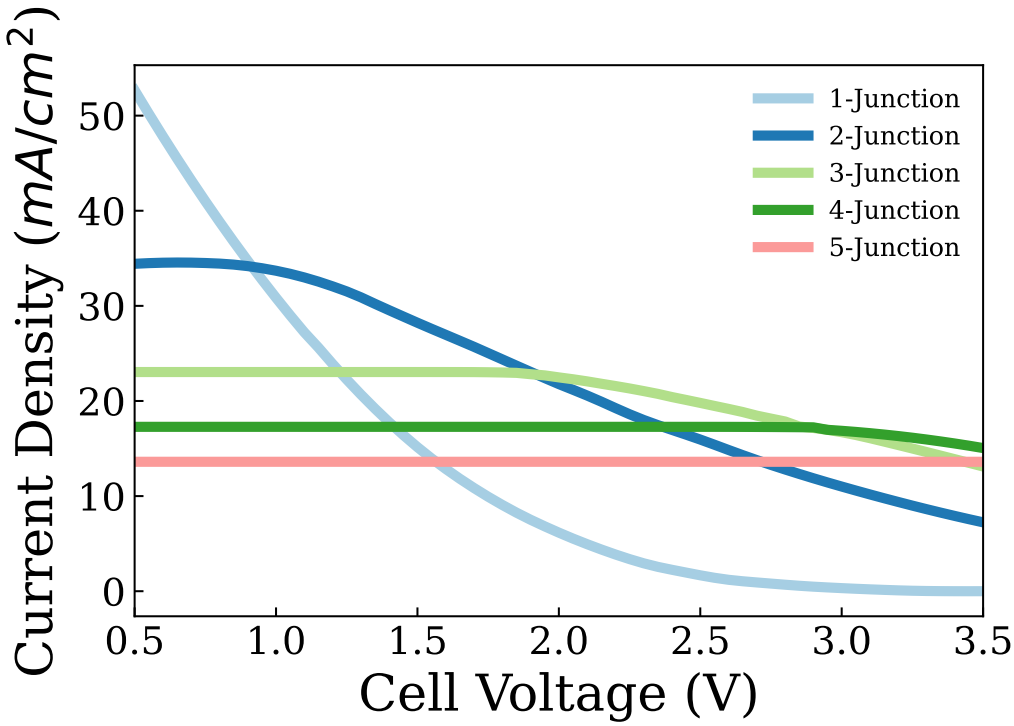

Figure 2. JV characteristics of ideal multijunction light absorbers showing the maximum current density of the light absorbers at any given cell voltage for an electrochemical reaction.

Table 1 presents the determination of thermoneutral potentials for ECR and MOR using Equation (3). It is essential to note that the assessment of thermoneutral potentials considers these reactions under near-ideal conditions, assuming adiabatic reactions and higher potential than equilibrium due to no ohmic or Nernstian losses, which can be experimentally determined.

Table 1. Thermoneutral potentials of ECR and MOR to methanol.

	Reaction	e	ΔH^0 (kJ mol^{-1})	V_{th} (V)
ECR	$CO_2 + 2H_2O \rightarrow CH_3OH + \frac{3}{2}O_2$	6	728.74	1.259
MOR	$CH_4 + H_2O \rightarrow CH_3OH + H_2$	2	121.94	0.632

With both the JV characteristics and thermoneutral potentials calculated, the STF efficiency for methanol production through ECR and MOR can be calculated using Equation (4). The maximum current density obtained from an ideal light absorber for a given ideal electrochemical reaction will be at the thermoneutral potential of the reaction. Figure 3 depicts the STF efficiency of methanol production for multijunction light absorbers through ECR and MOR routes.

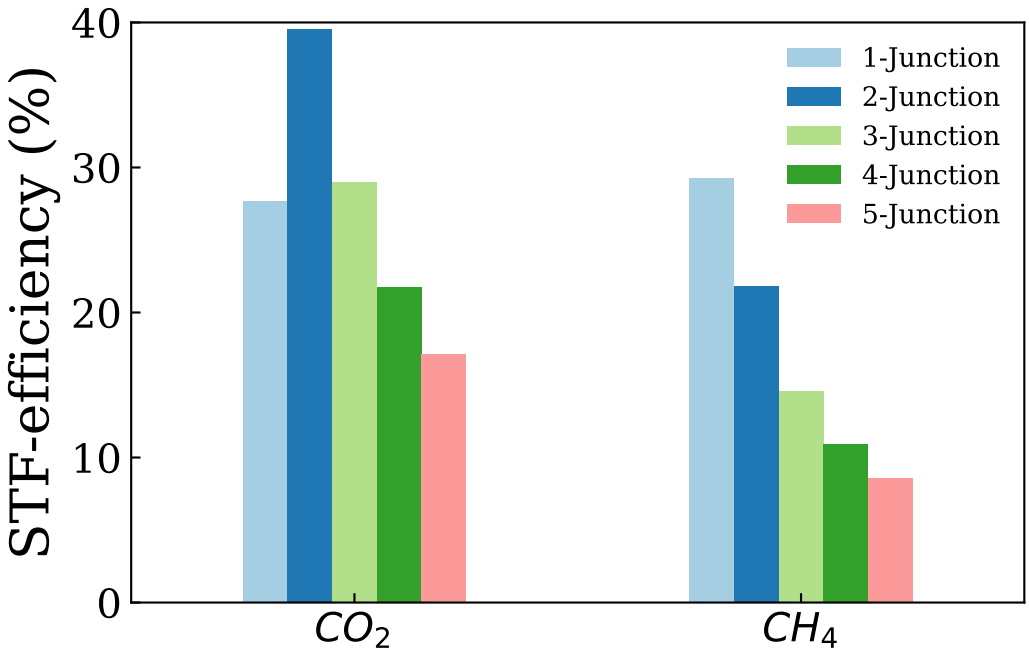

Figure 3. STF efficiency of methanol production using ideal multi-junction light absorbers and thermoneutral ECR and MOR.

ECR with a higher thermoneutral potential demonstrates the highest efficiency at 39.54% and 29.01% for double and triple junction light absorbers, respectively. Meanwhile, MOR exhibits the highest efficiencies at 29.27% and 21.83% for single and double junction light absorbers, respectively. The variation in STF efficiencies between each route for the same light absorbers arises from differences in thermoneutral potentials. STF efficiencies are lower for higher-order junction light absorbers due to poor matching of current densities among the junctions, as depicted in Figure 2. It is also noteworthy that leaves of plants contain two photosystems that function akin to a double junction light absorber, optimizing sunlight utilization for photosynthesis [24].

After evaluating the thermodynamic limits of ECR and MOR for methanol production, it is crucial to translate these findings into more realistic conditions. Figure 4A presents a comparison of the JV characteristics of a state-of-the-art triple junction light absorber (InGaP/GaAs/Ge) with the ideal triple junction light absorber. The significant disparity between these JV curves stems from extrinsic losses such as light reflection, contact shadowing, series resistance, inefficient collection of electrons and holes, nonradiative recombination, and temperature rise. Consequently, the real triple junction light absorber exhibits a lower maximum current density and a reduced stable current density over a narrower range of electrochemical load. Moreover, to enhance its utility across a broader range of operating potentials, these light absorbers can be connected in series. Connecting

two of these real light absorbers in series expands the operating voltage range but at the expense of decreased maximum current density as seen in Figure 4B. It is pertinent to note that the term "current density" in the context of light absorbers implies that the current is measured per unit area of the light absorber. The light absorber area can always be increased to match the higher currents required to operate more realistic electrochemical systems. Presently, our capabilities are constrained by the efficiency of today's light absorbers, although electrochemical cells have progressed to a higher TRL for ECR (and to some extent, MOR). Ongoing research endeavors can continuously improve light absorber efficiency to reduce material costs in the future while still matching the currents of an electrochemical system by augmenting the area of the light absorbers utilized today.

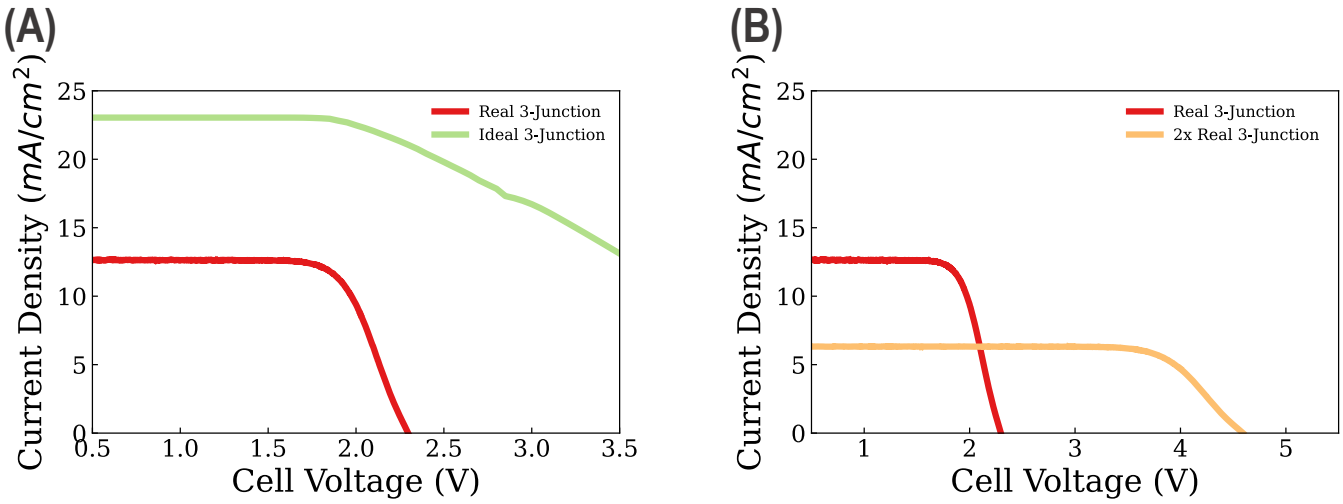

Figure 4. (**A**) JV characteristics of a real light absorber compared to an ideal light absorber. (**B**) JV characteristics of a real light absorber compared to 2 real light absorbers connected in series.

After comprehending the JV characteristics of a realistic light absorber, the next step is to consider non-ideal, realistic electrochemical reactions to evaluate the STF efficiencies of ECR and MOR for methanol production. Table 2 presents literature works on ECR and MOR to methanol. It is evident that significantly more progress has been made from ECR to methanol compared to MOR. Despite MOR having a much lower thermoneutral potential than ECR, it is kinetically challenging due to the non-polar, stable, and insoluble nature of CH_4 as a reactant. There may be more fundamental efforts needed to develop more efficient MOR electrochemical systems before it can go to higher TRL levels. However, another attractive intermediate route that has garnered attention lies between the two reactions considered here. A tandem approach of reducing CO_2 to CO which is already at high TRL levels followed by utilizing green H_2 to perform CO hydrogenation, yielding green methanol [64]. The utilization of green H_2 in the subsequent CO hydrogenation step ensures the overall environmental sustainability of the process. Green H_2 is produced through renewable energy sources, such as wind or solar, or even as a byproduct of ECR avoiding the carbon footprint associated with conventional hydrogen production methods. While the tandem electrochemical CO_2-to-CO and green methanol production pathway shows promise, several challenges need to be addressed. These include optimizing catalyst stability, improving energy efficiency, and scaling up the process for industrial applications. Furthermore, the economic viability of the overall system needs careful consideration. Deeper insight into this process may become a separate study on its own, therefore, we acknowledge the potential of tandem approach while focusing on ECR and MOR for the scope of this work.

The potentials reported in Table 2 correspond to the working electrode potentials, unlike the total cell potentials used in the calculations depicted in the preceding figures. Consequently, it is reasonable to assume that the total cell potentials would exceed the reported values in this table. Bearing this in mind, we varied the overpotential to ~2 volts

above the thermoneutral potential to evaluate the STF efficiency under realistic conditions, as illustrated in Figure 5A. In the case of ideal light absorbers, as the overpotential increases, the most efficient light absorber transitions from double to triple junction. However, due to extrinsic losses, the realistic efficiency remains around 20% at the highest overpotentials.

Table 2. Literature highlights for the performance of ECR and MOR to methanol.

	Catalyst	Electrolyte	Applied Potential (V)	Methanol Current Density (mA/cm^2)	Faradaic Efficiency (%)	References
CO_2	$CuGa_2$ (GDE)	CO_2 gas with 1 M KOH	−0.3 vs. RHE	21.4	77.26	[65]
	RuO_2/TiO_2 nanotubes (NTs)	0.5 M $NaHCO_3$	−0.8 vs. SCE	1.2	60.5	[66]
	PtZn nano-alloys	0.1 M $NaHCO_3$	−0.90 vs. RHE	3.75	81.4	[67]
	n-GaAs-crystal-(111)As	0.2 M Na_2SO_4	−1.20 to −1.40 vs. SCE	0.16–0.2	100	[68]
	$Pd_{83}Cu_{17}$ bimetallic aerogel	25 mol% [Bmim]BF_4 and 75 mol% water	−2.1 vs. Ag/Ag+	31.8	80	[69]
	Pre-oxidized Cu foil (1 h, 130 °C)	0.5 M $KHCO_3$	−0.9 vs. SCE	0.069	33.36	[70]
	RuO_2:TiO_2 (35:65)	0.05 M H_2SO_4	−0.05 vs. SCE	0.061	76	[71]
	$Cu_{1.63}Se_{0.33}$	[Bmim]PF_6 (30 wt %)/ CH_3CN/H_2O	−2.1 V vs. Ag/Ag+	30	80	[72]
CH_4	TiO_2-RuO_2	0.1 M Na_2SO_4	2.1 vs. SCE	13	30	[73]
	V_2O_5-SnO_2	$Sn_{0.9}In_{0.1}P_2O_7$	0.9	4	61.4	[74]
	$TiO_2/RuO_2/V_2O_5$	0.1 M Na_2SO_4	2.0 V vs. SCE	-	56	[75]
	3.0 NiO/Ni	0.1 M NaOH	1.40 V vs. RHE	3.0	14	[42]
	Cu-Ti	1 M KCl	3.07 V vs. RHE	6.24	16	[40]
	Cu-Ti	0.1 M KH_2PO_4-K_2HPO_4	2.15 V vs. RHE	0.3	7	[39]

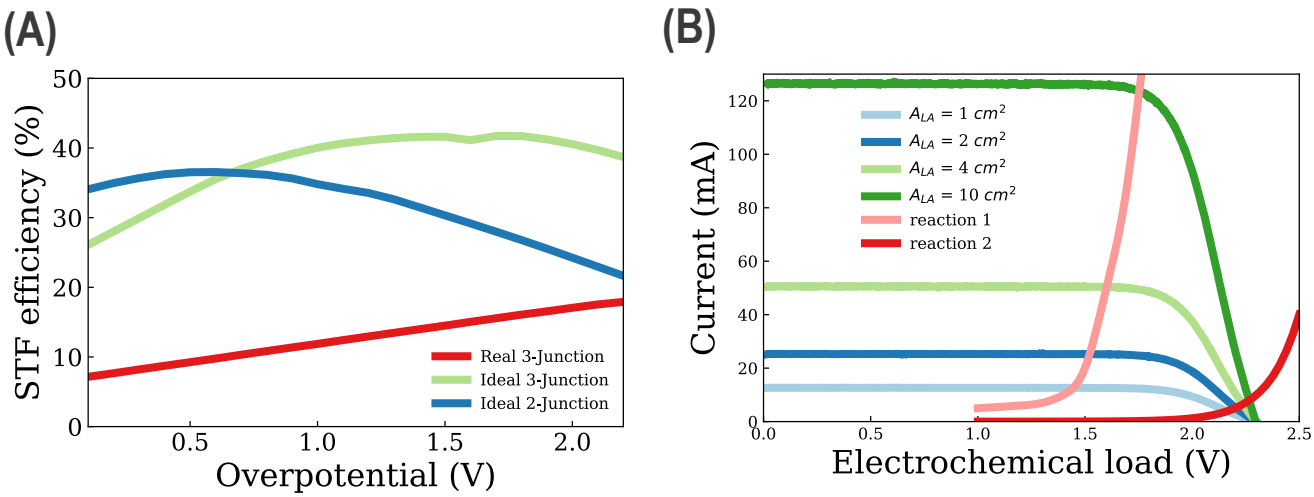

Figure 5. (**A**) STF efficiency comparing realistic ECR and MOR systems with real and ideal light absorbers. (**B**) Effect of area on the operating point of integrated PV–EC systems.

Under realistic conditions, it is important to understand how a PV–EC system operates when the two individual components -PV light absorber and electrochemical cell- are integrated. This is highlighted in Figure 5B, where we see the JV characteristics of a realistic triple junction light absorber (from Figure 4A) of various light absorber areas along with 2 hypothetical electrochemical reactions. From this figure it can be seen that a PV–EC integrated system will operate where the light absorber and the electrochemical reaction JV curves intersect, which is also evident in some recent experimental work on integrated

PV–EC systems [76,77]. As the area increases, the current at any given potential also increases linearly for the light absorber. The hypothetical electrochemical reaction 1, in this case, appears to be an efficient reaction where the EC system is able to drive higher currents at lower voltages. For such efficient reactions, the PV–EC system is limited by the light absorber JV characteristics. Hence, increasing the area of a light absorber can increase the operating current and consequently, increase the STF efficiency. On the other hand, the hypothetical electrochemical reaction 2 is an inefficient reaction. Here, the EC system appears to have sluggish JV curve and increasing the light absorber area will not increase the current and the STF efficiency significantly. In this case, increasing the area of the electrocatalyst can help reach higher operating currents leading to higher STF efficiency. It should be noted that scaling both PV and EC systems is a non-trivial task and may lead to emergent phenomena, such as uneven temperature distribution and localized current distribution [78], and may require various engineering controls to mitigate scaling effects. Alternatively, optimizing this EC reaction to make it more efficient like reaction 1, would also be beneficial. This analogy can be extrapolated to ECR and MOR as well, since ECR has higher TRL (resembling reaction 1), and MOR has a lower TRL (resembling reaction 2). The design principles discussed above can be directly applied to integrated PV–EC systems for ECR and MOR. The insights from Figure 5B provide valuable guidance for designing integrated PV–EC systems tailored for specific electrochemical reactions, facilitating informed decision-making and optimization strategies. By leveraging these insights, researchers can navigate the design space effectively, advancing the development and deployment of efficient solar-driven electrochemical systems for sustainable energy conversion and storage applications.

4. Conclusions

The exploration of solar-driven electrochemical processes for methanol production presents a promising avenue towards sustainable energy solutions. This study delves into the integration of electrochemistry with renewable energy, particularly solar power, to drive efficient chemical reactions for methanol synthesis. The analysis highlights the feasibility and potential of both electrochemical reduction (ECR) of CO_2 and methane oxidation reaction (MOR) as pathways for methanol production. ECR is currently particularly promising, exhibiting higher efficiencies and technological readiness levels compared to MOR. However, challenges persist in both processes, including catalyst stability and reaction kinetics. Our findings highlight the importance of considering realistic conditions in evaluating solar-to-fuel (STF) efficiencies. While ideal scenarios demonstrate significant potential, extrinsic losses and practical limitations temper the achievable efficiencies. The advances in light absorber technology and electrochemical systems offer avenues for continual improvement and optimization and demonstrate a promise to compensate for the higher cost of this decoupled electrochemical system. The integration of PV light absorbers with electrochemical cells in realistic conditions necessitates a nuanced understanding of their operational dynamics, as explained by the intersection of JV characteristics of these individual systems to determine the operating point of an integrated PV–EC system. This integration shows the significance of optimizing light absorber and electrochemical reaction geometric areas to enhance system performance and STF efficiency. Efficient electrochemical reactions highlight the importance of maximizing light absorber areas, while inefficient electrochemical reactions necessitate focus on electrocatalyst areas or urges the field to direct efforts toward developing more efficient EC systems. The principles delineated herein, furnish a framework for tailored PV–EC system designs, guiding optimization strategies and informed decision-making. By leveraging these insights, researchers can direct the development and deployment of solar-driven electrochemical systems towards sustainable energy conversion and storage applications. Looking ahead, future research efforts should focus on addressing key challenges in catalyst design, reaction kinetics, and system optimization to further enhance STF efficiencies. Additionally, efforts to integrate solar-driven electrochemical processes into larger energy systems and industrial applications are essential for practical implementation.

Collaboration across disciplines, including material science, electrochemistry, and renewable energy engineering, will be crucial in driving innovation and fostering the transition towards a sustainable methanol economy. In conclusion, this study provides insights into the thermodynamic and practical considerations of solar-driven electrochemical methanol production. By elucidating the complexities and opportunities inherent in ECR and MOR pathways, we pave the way for informed decision-making and targeted research efforts aimed at realizing the full potential of solar-driven methanol synthesis in shaping a cleaner and more sustainable energy future.

Author Contributions: Conceptualization, A.P. (Aaditya Pendse) and A.P. (Aditya Prajapati); methods, A.P. (Aditya Prajapati); analysis and insights, A.P. (Aaditya Pendse) and A.P. (Aditya Prajapati); literature data curation, A.P. (Aaditya Pendse); writing-original draft preparation, A.P. (Aaditya Pendse) and A.P. (Aditya Prajapati); writing-review and editing, A.P. (Aaditya Pendse) and A.P. (Aditya Prajapati). All authors have read and agreed to the published version of the manuscript.

Funding: This research received no external funding.

Acknowledgments: This work was performed under the auspices of the U.S. Department of Energy by Lawrence Livermore National Laboratory under Contract DE-AC52-07NA27344 with IM release number LLNL-JRNL-860117.

Conflicts of Interest: The authors declare no conflict of interest.

References

1. Shah, W.U.H.; Hao, G.; Yan, H.; Zhu, N.; Yasmeen, R.; Dincă, G. Role of renewable, non-renewable energy consumption and carbon emission in energy efficiency and productivity change: Evidence from G20 economies. *Geosci. Front.* **2023**, 101631. [CrossRef]
2. *Bp Statistical Review of World Energy*, 71st ed.; Pureprint Group Limited: London, UK, 2022.
3. Sonthalia, A.; Kumar, N.; Tomar, M.; Edwin Geo, V.; Thiyagarajan, S.; Pugazhendhi, A. Moving ahead from hydrogen to methanol economy: Scope and challenges. *Clean Technol. Environ. Policy* **2021**, *25*, 551–575. [CrossRef]
4. Li, J.; Zhu, X.; Djilali, N.; Yang, Y.; Ye, D.; Chen, R.; Liao, Q. Comparative well-to-pump assessment of fueling pathways for zero-carbon transportation in China: Hydrogen economy or methanol economy? *Renew. Sustain. Energy Rev.* **2022**, *169*, 112935. [CrossRef]
5. Filosa, C.; Gong, X.; Bavykina, A.; Chowdhury, A.D.; Gallo, J.M.R.; Gascon, J. Enabling the Methanol Economy: Opportunities and Challenges for Heterogeneous Catalysis in the Production of Liquid Fuels via Methanol. *Acc. Chem. Res.* **2023**, *56*, 3492–3503. [CrossRef]
6. Olah, G.A.; Goeppert, A.; Prakash, G.S. *Beyond Oil and Gas: The Methanol Economy*; John Wiley & Sons: Hoboken, NJ, USA, 2011.
7. Dalena, F.; Senatore, A.; Marino, A.; Gordano, A.; Basile, M.; Basile, A. Methanol production and applications: An overview. In *Methanol*; Elsevier: Amsterdam, The Netherlands, 2018; pp. 3–28.
8. Alias, M.; Kamarudin, S.; Zainoodin, A.; Masdar, M. Active direct methanol fuel cell: An overview. *Int. J. Hydrogen Energy* **2020**, *45*, 19620–19641. [CrossRef]
9. Cox, C.R.; Lee, J.Z.; Nocera, D.G.; Buonassisi, T. Ten-percent solar-to-fuel conversion with nonprecious materials. *Proc. Natl. Acad. Sci. USA* **2014**, *111*, 14057–14061. [CrossRef] [PubMed]
10. Park, H.; Park, I.J.; Lee, M.G.; Kwon, K.C.; Hong, S.-P.; Kim, D.H.; Lee, S.A.; Lee, T.H.; Kim, C.; Moon, C.W. Water splitting exceeding 17% solar-to-hydrogen conversion efficiency using solution-processed Ni-based electrocatalysts and perovskite/Si tandem solar cell. *ACS Appl. Mater. Interfaces* **2019**, *11*, 33835–33843. [CrossRef]
11. Kobayashi, H.; Sato, N.; Orita, M.; Kuang, Y.; Kaneko, H.; Minegishi, T.; Yamada, T.; Domen, K. Development of highly efficient $CuIn_{0.5}Ga_{0.5}Se_2$-based photocathode and application to overall solar driven water splitting. *Energy Environ. Sci.* **2018**, *11*, 3003–3009. [CrossRef]
12. Pan, L.; Kim, J.H.; Mayer, M.T.; Son, M.-K.; Ummadisingu, A.; Lee, J.S.; Hagfeldt, A.; Luo, J.; Grätzel, M. Boosting the performance of Cu_2O photocathodes for unassisted solar water splitting devices. *Nat. Catal.* **2018**, *1*, 412–420. [CrossRef]
13. Kato, N.; Mizuno, S.; Shiozawa, M.; Nojiri, N.; Kawai, Y.; Fukumoto, K.; Morikawa, T.; Takeda, Y. A large-sized cell for solar-driven CO_2 conversion with a solar-to-formate conversion efficiency of 7.2%. *Joule* **2021**, *5*, 687–705. [CrossRef]
14. Villa, K.; Galán-Mascarós, J.R. Nanostructured photocatalysts for the production of methanol from methane and water. *ChemSusChem* **2021**, *14*, 2023–2033. [CrossRef] [PubMed]
15. Zeng, Y.; Tang, Z.; Wu, X.; Huang, A.; Luo, X.; Xu, G.Q.; Zhu, Y.; Wang, S.L. Photocatalytic oxidation of methane to methanol by tungsten trioxide-supported atomic gold at room temperature. *Appl. Catal. B Environ.* **2022**, *306*, 120919. [CrossRef]
16. Sharma, P.; Kumar, S.; Tomanec, O.; Petr, M.; Zhu Chen, J.; Miller, J.T.; Varma, R.S.; Gawande, M.B.; Zbořil, R. Carbon nitride-based ruthenium single atom photocatalyst for CO_2 reduction to methanol. *Small* **2021**, *17*, 2006478. [CrossRef]
17. Ding, J.; Tang, Q.; Fu, Y.; Zhang, Y.; Hu, J.; Li, T.; Zhong, Q.; Fan, M.; Kung, H.H. Core–shell covalently linked graphitic carbon nitride–melamine–resorcinol–formaldehyde microsphere polymers for efficient photocatalytic CO_2 reduction to methanol. *J. Am. Chem. Soc.* **2022**, *144*, 9576–9585. [CrossRef] [PubMed]

18. McDaniel, A.H.; Ambrosini, A.; Coker, E.N.; Miller, J.E.; Chueh, W.C.; O'Hayre, R.; Tong, J. Nonstoichiometric perovskite oxides for solar thermochemical H_2 and CO production. *Energy Procedia* **2014**, *49*, 2009–2018. [CrossRef]
19. Scheffe, J.R.; Steinfeld, A. Oxygen exchange materials for solar thermochemical splitting of H_2O and CO_2: A review. *Mater. Today* **2014**, *17*, 341–348. [CrossRef]
20. Frese, K.; Leach, S. Electrochemical reduction of carbon dioxide to methane, methanol, and CO on Ru electrodes. *J. Electrochem. Soc.* **1985**, *132*, 259. [CrossRef]
21. Hori, Y.; Murata, A.; Takahashi, R. Formation of hydrocarbons in the electrochemical reduction of carbon dioxide at a copper electrode in aqueous solution. *J. Chem. Soc. Faraday Trans. 1 Phys. Chem. Condens. Phases* **1989**, *85*, 2309–2326. [CrossRef]
22. Kaneco, S.; Katsumata, H.; Suzuki, T.; Ohta, K. Electrochemical reduction of CO_2 on Cu electrode in methanol at low temperature. In *Utilization of Greenhouse Gases*; ACS Publications: Washington, DC, USA, 2003.
23. Chang, X.; Wang, T.; Zhang, P.; Wei, Y.; Zhao, J.; Gong, J. Stable aqueous photoelectrochemical CO_2 reduction by a Cu_2O dark cathode with improved selectivity for carbonaceous products. *Angew. Chem. Int. Ed.* **2016**, *55*, 8840–8845. [CrossRef]
24. Kong, Q.; Kim, D.; Liu, C.; Yu, Y.; Su, Y.; Li, Y.; Yang, P. Directed assembly of nanoparticle catalysts on nanowire photoelectrodes for photoelectrochemical CO_2 reduction. *Nano Lett.* **2016**, *16*, 5675–5680. [CrossRef]
25. Nakada, A.; Koike, K.; Nakashima, T.; Morimoto, T.; Ishitani, O. Photocatalytic CO_2 reduction to formic acid using a Ru (II)–Re (I) supramolecular complex in an aqueous solution. *Inorg. Chem.* **2015**, *54*, 1800–1807. [CrossRef]
26. Yu, J.; Low, J.; Xiao, W.; Zhou, P.; Jaroniec, M. Enhanced photocatalytic CO_2-reduction activity of anatase TiO_2 by coexposed {001} and {101} facets. *J. Am. Chem. Soc.* **2014**, *136*, 8839–8842. [CrossRef] [PubMed]
27. Nitopi, S.; Bertheussen, E.; Scott, S.B.; Liu, X.; Engstfeld, A.K.; Horch, S.; Seger, B.; Stephens, I.E.; Chan, K.; Hahn, C. Progress and perspectives of electrochemical CO_2 reduction on copper in aqueous electrolyte. *Chem. Rev.* **2019**, *119*, 7610–7672. [CrossRef] [PubMed]
28. Jouny, M.; Luc, W.; Jiao, F. General techno-economic analysis of CO_2 electrolysis systems. *Ind. Eng. Chem. Res.* **2018**, *57*, 2165–2177. [CrossRef]
29. Albo, J.; Alvarez-Guerra, M.; Castaño, P.; Irabien, A. Towards the electrochemical conversion of carbon dioxide into methanol. *Green Chem.* **2015**, *17*, 2304–2324. [CrossRef]
30. Ganesh, I. Conversion of carbon dioxide into methanol—A potential liquid fuel: Fundamental challenges and opportunities (a review). *Renew. Sustain. Energy Rev.* **2014**, *31*, 221–257. [CrossRef]
31. Shi, C.; Chan, K.; Yoo, J.S.; Nørskov, J.K. Barriers of electrochemical CO_2 reduction on transition metals. *Org. Process Res. Dev.* **2016**, *20*, 1424–1430. [CrossRef]
32. Frese, K.; Canfield, D. Reduction of CO_2 on n-GaAs electrodes and selective methanol synthesis. *J. Electrochem. Soc.* **1984**, *131*, 2518. [CrossRef]
33. Inoue, T.; Fujishima, A.; Konishi, S.; Honda, K. Photoelectrocatalytic reduction of carbon dioxide in aqueous suspensions of semiconductor powders. *Nature* **1979**, *277*, 637–638. [CrossRef]
34. Barton, E.E.; Rampulla, D.M.; Bocarsly, A.B. Selective solar-driven reduction of CO_2 to methanol using a catalyzed p-GaP based photoelectrochemical cell. *J. Am. Chem. Soc.* **2008**, *130*, 6342–6344. [CrossRef]
35. Rajeshwar, K.; de Tacconi, N.R.; Ghadimkhani, G.; Chanmanee, W.; Janáky, C. Tailoring copper oxide semiconductor nanorod arrays for photoelectrochemical reduction of carbon dioxide to methanol. *ChemPhysChem* **2013**, *14*, 2251–2259. [CrossRef]
36. Yuan, J.; Hao, C. Solar-driven photoelectrochemical reduction of carbon dioxide to methanol at CuInS2 thin film photocathode. *Sol. Energy Mater. Sol. Cells* **2013**, *108*, 170–174. [CrossRef]
37. World's Largest CO_2-To-Methanol Plant Starts Production. Available online: https://www.carbonrecycling.is/news-media/worlds-largest-co2-to-methanol-plant-starts-production (accessed on 25 February 2024).
38. Habibic, A. Yale-Based Start-Up Converts Captured CO_2 into Methanol. Available online: https://www.offshore-energy.biz/yale-based-start-up-converts-captured-co2-into-methanol/ (accessed on 25 February 2024).
39. Prajapati, A.; Collins, B.A.; Goodpaster, J.D.; Singh, M.R. Fundamental insight into electrochemical oxidation of methane towards methanol on transition metal oxides. *Proc. Natl. Acad. Sci. USA* **2021**, *118*, e2023233118. [CrossRef] [PubMed]
40. Prajapati, A.; Sartape, R.; Kani, N.C.; Gauthier, J.A.; Singh, M.R. Chloride-Promoted High-Rate Ambient Electrooxidation of Methane to Methanol on Patterned Cu–Ti Bimetallic Oxides. *ACS Catal.* **2022**, *12*, 14321–14329. [CrossRef]
41. Spinner, N.; Mustain, W.E. Electrochemical methane activation and conversion to oxygenates at room temperature. *ECS Trans.* **2013**, *53*, 1. [CrossRef]
42. Song, Y.; Zhao, Y.; Nan, G.; Chen, W.; Guo, Z.; Li, S.; Tang, Z.; Wei, W.; Sun, Y. Electrocatalytic oxidation of methane to ethanol via NiO/Ni interface. *Appl. Catal. B Environ.* **2020**, *270*, 118888. [CrossRef]
43. Kim, R.S.; Surendranath, Y. Electrochemical reoxidation enables continuous methane-to-methanol catalysis with aqueous Pt salts. *ACS Cent. Sci.* **2019**, *5*, 1179–1186. [CrossRef]
44. Ma, M.; Jin, B.J.; Li, P.; Jung, M.S.; Kim, J.I.; Cho, Y.; Kim, S.; Moon, J.H.; Park, J.H. Ultrahigh electrocatalytic conversion of methane at room temperature. *Adv. Sci.* **2017**, *4*, 1700379. [CrossRef]
45. Omasta, T.J.; Rigdon, W.A.; Lewis, C.A.; Stanis, R.J.; Liu, R.; Fan, C.Q.; Mustain, W.E. Two pathways for near room temperature electrochemical conversion of methane to methanol. *ECS Trans.* **2015**, *66*, 129. [CrossRef]
46. Lee, J.; Yang, J.; Moon, J.H. Solar cell-powered electrochemical methane-to-methanol conversion with CuO/CeO_2 catalysts. *ACS Energy Lett.* **2021**, *6*, 893–899. [CrossRef]

47. Bonchio, M.; Bonin, J.; Ishitani, O.; Lu, T.-B.; Morikawa, T.; Morris, A.J.; Reisner, E.; Sarkar, D.; Toma, F.M.; Robert, M. Best practices for experiments and reporting in photocatalytic CO_2 reduction. *Nat. Catal.* **2023**, *6*, 657–665. [CrossRef]
48. Seger, B.; Robert, M.; Jiao, F. Best practices for electrochemical reduction of carbon dioxide. *Nat. Sustain.* **2023**, *6*, 236–238. [CrossRef]
49. Prajapati, A. Electrochemical Routes for Upgrading Carbon-Based Greenhouse Gases. Ph.D. Thesis, University of Illinois, Chicago, IL, USA, 2022.
50. Sahara, G.; Kumagai, H.; Maeda, K.; Kaeffer, N.; Artero, V.; Higashi, M.; Abe, R.; Ishitani, O. Photoelectrochemical reduction of CO_2 coupled to water oxidation using a photocathode with a Ru (II)–Re (I) complex photocatalyst and a CoOx/TaON photoanode. *J. Am. Chem. Soc.* **2016**, *138*, 14152–14158. [CrossRef]
51. Schreier, M.; Curvat, L.; Giordano, F.; Steier, L.; Abate, A.; Zakeeruddin, S.M.; Luo, J.; Mayer, M.T.; Grätzel, M. Efficient photosynthesis of carbon monoxide from CO_2 using perovskite photovoltaics. *Nat. Commun.* **2015**, *6*, 7326. [CrossRef]
52. Sekimoto, T.; Shinagawa, S.; Uetake, Y.; Noda, K.; Deguchi, M.; Yotsuhashi, S.; Ohkawa, K. Tandem photo-electrode of InGaN with two Si pn junctions for CO_2 conversion to HCOOH with the efficiency greater than biological photosynthesis. *Appl. Phys. Lett.* **2015**, *106*, 073902. [CrossRef]
53. Zhou, X.; Liu, R.; Sun, K.; Chen, Y.; Verlage, E.; Francis, S.A.; Lewis, N.S.; Xiang, C. Solar-driven reduction of 1 atm of CO_2 to formate at 10% energy-conversion efficiency by use of a TiO_2-protected III–V tandem photoanode in conjunction with a bipolar membrane and a Pd/C cathode. *ACS Energy Lett.* **2016**, *1*, 764–770. [CrossRef]
54. He, J.; Janaky, C. Recent advances in solar-driven carbon dioxide conversion: Expectations versus reality. *ACS Energy Lett.* **2020**, *5*, 1996–2014. [CrossRef] [PubMed]
55. Tan, Y.C.; Quek, W.K.; Kim, B.; Sugiarto, S.; Oh, J.; Kai, D. Pitfalls and protocols: Evaluating catalysts for CO_2 reduction in electrolyzers based on gas diffusion electrodes. *ACS Energy Lett.* **2022**, *7*, 2012–2023. [CrossRef]
56. Tan, J.; Kang, B.; Kim, K.; Kang, D.; Lee, H.; Ma, S.; Jang, G.; Lee, H.; Moon, J. Hydrogel protection strategy to stabilize water-splitting photoelectrodes. *Nat. Energy* **2022**, *7*, 537–547. [CrossRef]
57. Xiao, M.; Wang, Z.; Maeda, K.; Liu, G.; Wang, L. Addressing the stability challenge of photo (electro) catalysts towards solar water splitting. *Chem. Sci.* **2023**, *14*, 3415–3427. [CrossRef]
58. Garg, S.; Li, M.; Weber, A.Z.; Ge, L.; Li, L.; Rudolph, V.; Wang, G.; Rufford, T.E. Advances and challenges in electrochemical CO_2 reduction processes: An engineering and design perspective looking beyond new catalyst materials. *J. Mater. Chem. A* **2020**, *8*, 1511–1544. [CrossRef]
59. Liang, S.; Altaf, N.; Huang, L.; Gao, Y.; Wang, Q. Electrolytic cell design for electrochemical CO_2 reduction. *J. CO_2 Util.* **2020**, *35*, 90–105. [CrossRef]
60. Garg, S.; Xie, Z.; Chen, J.G. Tandem reactors and reactions for CO_2 conversion. *Nat. Chem. Eng.* **2024**, *1*, 139–148. [CrossRef]
61. Kim, B.; Tan, Y.C.; Ryu, Y.; Jang, K.; Abbas, H.G.; Kang, T.; Choi, H.; Lee, K.-S.; Park, S.; Kim, W. Trace-level cobalt dopants enhance CO_2 electroreduction and ethylene formation on copper. *ACS Energy Lett.* **2023**, *8*, 3356–3364. [CrossRef]
62. Pan, F.; Yang, Y. Designing CO_2 reduction electrode materials by morphology and interface engineering. *Energy Environ. Sci.* **2020**, *13*, 2275–2309. [CrossRef]
63. Prajapati, A.; Singh, M.R. Assessment of artificial photosynthetic systems for integrated carbon capture and conversion. *ACS Sustain. Chem. Eng.* **2019**, *7*, 5993–6003. [CrossRef]
64. Kim, B.; Seong, H.; Song, J.T.; Kwak, K.; Song, H.; Tan, Y.C.; Park, G.; Lee, D.; Oh, J. Over a 15.9% solar-to-CO conversion from dilute CO_2 streams catalyzed by gold nanoclusters exhibiting a high CO_2 binding affinity. *ACS Energy Lett.* **2019**, *5*, 749–757. [CrossRef]
65. Bagchi, D.; Raj, J.; Singh, A.K.; Cherevotan, A.; Roy, S.; Manoj, K.S.; Vinod, C.; Peter, S.C. Structure-Tailored Surface Oxide on Cu–Ga Intermetallics Enhances CO_2 Reduction Selectivity to Methanol at Ultralow Potential. *Adv. Mater.* **2022**, *34*, 2109426. [CrossRef] [PubMed]
66. Qu, J.; Zhang, X.; Wang, Y.; Xie, C. Electrochemical reduction of CO_2 on RuO_2/TiO_2 nanotubes composite modified Pt electrode. *Electrochim. Acta* **2005**, *50*, 3576–3580. [CrossRef]
67. Payra, S.; Shenoy, S.; Chakraborty, C.; Tarafder, K.; Roy, S. Structure-sensitive electrocatalytic reduction of CO_2 to methanol over carbon-supported intermetallic PtZn nano-alloys. *ACS Appl. Mater. Interfaces* **2020**, *12*, 19402–19414. [CrossRef]
68. Canfield, D.; Frese, K., Jr. Reduction of carbon dioxide to methanol on n-and p-GaAs and p-InP. Effect of crystal face, electrolyte and current density. *J. Electrochem. Soc.* **1983**, *130*, 1772–1773. [CrossRef]
69. Lu, L.; Sun, X.; Ma, J.; Yang, D.; Wu, H.; Zhang, B.; Zhang, J.; Han, B. Highly efficient electroreduction of CO_2 to methanol on palladium–copper bimetallic aerogels. *Angew. Chem.* **2018**, *130*, 14345–14349. [CrossRef]
70. Frese, K.W. Electrochemical reduction of CO_2 at intentionally oxidized copper electrodes. *J. Electrochem. Soc.* **1991**, *138*, 3338. [CrossRef]
71. Bandi, A. Electrochemical reduction of carbon dioxide on conductive metallic oxides. *J. Electrochem. Soc.* **1990**, *137*, 2157. [CrossRef]
72. Yang, D.; Zhu, Q.; Chen, C.; Liu, H.; Liu, Z.; Zhao, Z.; Zhang, X.; Liu, S.; Han, B. Selective electroreduction of carbon dioxide to methanol on copper selenide nanocatalysts. *Nat. Commun.* **2019**, *10*, 677. [CrossRef] [PubMed]
73. Rocha, R.S.; Camargo, L.M.; Lanza, M.R.V.; Bertazzoli, R. A Feasibility Study of the Electro-recycling of Greenhouse Gases: Design and Characterization of a (TiO_2/RuO_2)/PTFE Gas Diffusion Electrode for the Electrosynthesis of Methanol from Methane. *Electrocatalysis* **2010**, *1*, 224–229. [CrossRef]
74. Lee, B.; Hibino, T. Efficient and selective formation of methanol from methane in a fuel cell-type reactor. *J. Catal.* **2011**, *279*, 233–240. [CrossRef]

75. Rocha, R.S.; Reis, R.M.; Lanza, M.R.; Bertazzoli, R. Electrosynthesis of methanol from methane: The role of V_2O_5 in the reaction selectivity for methanol of a $TiO_2/RuO_2/V_2O_5$ gas diffusion electrode. *Electrochim. Acta* **2013**, *87*, 606–610. [CrossRef]
76. Kani, N.C.; Gauthier, J.A.; Prajapati, A.; Edgington, J.; Bordawekar, I.; Shields, W.; Shields, M.; Seitz, L.C.; Singh, A.R.; Singh, M.R. Solar-driven electrochemical synthesis of ammonia using nitrate with 11% solar-to-fuel efficiency at ambient conditions. *Energy Environ. Sci.* **2021**, *14*, 6349–6359. [CrossRef]
77. Prajapati, A.; Kani, N.C.; Gauthier, J.A.; Sartape, R.; Xie, J.; Bessa, I.; Galante, M.T.; Leung, S.L.; Andrade, M.H.; Somich, R.T. CO_2-free high-purity ethylene from electroreduction of CO_2 with 4% solar-to-ethylene and 10% solar-to-carbon efficiencies. *Cell Rep. Phys. Sci.* **2022**, *3*, 101053. [CrossRef]
78. Goldman, M.; Prajapati, A.; Duoss, E.; Baker, S.; Hahn, C. Bridging Fundamental Science and Applied Science to Accelerate CO_2 Electrolyzer Scale up. *Curr. Opin. Electrochem.* **2023**, *39*, 101248. [CrossRef]